Inorg. Chem. **2006**, *45*, 10702–10711

Construction of Polyoxometalates-Based Coordination Polymers through Direct Incorporation between Polyoxometalates and the Voids in a 2D Network

Xiang-Jian Kong, Yan-Ping Ren, Pei-Qing Zheng, Yu-Xiang Long, La-Sheng Long,* Rong-Bin Huang, and Lan-Sun Zheng

State Key Laboratory of Physical Chemistry of Solid Surface, Key Laboratory of Analytical Sciences, Ministry of Education and Department of Chemistry, College of Chemistry and Chemical Engineering, Xiamen University, Xiamen 361005, China

Received September 3, 2006

A series of polyoxometalates (POMs)-based coordination polymers, namely, $\{[Cu(2,3\text{-}Me_2pz)(2,5\text{-}Me_2pz)_{0.5}]_4(SiW_{12}O_{40})(2,5\text{-}Me_2pz)\}_n$ (2,3-Me_2pz = 2,3-dimethylpyrazine; 2,5-Me_2pz = 2,5-dimethylpyrazine; **1**), $\{[Cu_2(4,4'\text{-bipy})_4(H_2O)_4](SiW_{12}O_{40})(H_2O)_{18}\}_n$ (4,4′-bipy = 4,4′-bipyridine; **2**), $\{[Cu(2\text{-Mepz})_{1.5}]_3(PMo_{12}O_{40})(H_2O)_{3.5}\}_n$ (2-Mepz = 2-methylpyrazine; **3**), $\{[Ag(2,3\text{-}Me_2pz)_{1.5}]_4(SiW_{12}O_{40})\}_n$ (**4**), $\{[Cu(pz)_{1.5}]_4(SiW_{12}O_{40})(H_2O)_3\}_n$ (pz = pyrazine; **5**), $\{[Cu(2,3\text{-}Me_2pz)_{1.5}]_4(SiW_{12}O_{40})\}_n$ (**6**), $\{[Cu(4,4'\text{-bipy})_{1.75}]_4(SiW_{12}O_{40})(H_2O)_2\}_n$ (**7**), and $\{[Cu_2(4,4'\text{-bipy})_4(H_2O)_4](SiW_{12}O_{40})(4,4'\text{-bipy})_2(H_2O)_4\}_n$ (**8**), were synthesized through direct incorporation between POMs and the voids of the 2D network. Crystal structural analysis reveals that the relationship between the size of the void of the 2D network and that of POMs is of key importance for successful synthesis of POMs-based open metal–organic frameworks. Guest replacement shows that the pore size of the framework constructed through direct incorporation between POMs and the voids of the 2D network is very sensitive to guest molecules.

Introduction

Open metal−organic frameworks, because of their pore size/shape and chemical functionality, controllable and adjustable, are regarded as promising materials for applications in catalysis, separation, gas storage, and molecular recognition.[1] Bearing unique properties and exhibiting a diverse compositional range, polyoxometalates (POMs) represent an outstanding class of molecular building blocks for the construction of such kinds of materials.[2] Owing to the large number of potential coordination sites and the relatively weak coordination ability of POMs, however, it is difficult for us to assemble 3D POMs-based coordination polymers,[2] especially POMs-based open metal−organic frameworks, based on their structural information under the guidance of the directionality of coordination bonding.[3] To overcome the difficulties encountered in the construction of POMs-based coordination polymers through the approach of covalently linking POMs with metal−organic units, Zubieta and co-workers[4] developed a new synthetic approach, that is, embedding POMs into the framework of the coordination polymers to construct 3D POMs-based coordination polymers. Here, we report the syntheses and crystal structures of a series of 3D POMs-based coordination polymers, namely, $\{[Cu(2,3\text{-}Me_2pz)(2,5\text{-}Me_2pz)_{0.5}]_4(SiW_{12}O_{40})(2,5\text{-}Me_2pz)\}_n$ (2,3-Me_2pz = 2,3-dimethylpyrazine; 2,5-Me_2pz = 2,5-dimethylpyrazine; **1**), $\{[Cu_2(4,4'\text{-bipy})_4(H_2O)_4](SiW_{12}O_{40})(H_2O)_{18}\}_n$ (4,4′-bipy = 4,4′-bipyridine; **2**), $\{[Cu(2\text{-Mepz})_{1.5}]_3$-

* To whom correspondence should be addressed. E-mail: lslong@jingxian.xmu.edu.cn. Fax: 86-592-2183047.

(1) Ozin, G. A.; Kuperman, A.; Stein, A. *Angew. Chem., Int. Ed. Engl.* **1989**, *28*, 359. Corma, A. *Chem. Rev.* **1997**, *97*, 2373. Seo, J. S.; Whang, D.; Lee, H.; Jun, S. I.; Oh, J.; Jeon, Y. J.; Kim, K. *Nature* **2000**, *404*, 982. Eddaoudi, M.; Moler, D. B.; Li, H.; Chen, B.; Reineke, T. M.; O'Keeffe, M.; Yaghi, O. M. *Acc. Chem. Res.* **2001**, *34*, 319. Moulton, B.; Zaworotko, M. J. *Chem. Rev.* **2001**, *101*, 1629. Yaghi, O. M.; O'Keeffe, M.; Ockwig, N. W.; Chae, H. K.; Eddaoudi, M.; Kim, J. *Nature* **2003**, *423*, 705. Bradshaw, D.; Claridge, J. B.; Cussen, E. J.; Prior, T. J.; Rosseinsky, M. J. *Acc. Chem. Res.* **2005**, *38*, 273. Matsuda, R.; Kitaura, R.; Kitagawa, S.; Kubota, Y.; Belosludov, R. V.; Kobayashi, T. C.; Sakamoto, H.; Chiba, T.; Takata, M.; Kawazoe, Y.; Mita, Y. *Nature* **2005**, *436*, 238.

(2) Lu, J.; Shen, E.-H.; Li, Y.-G.; Xiao, D.-R.; Wang, E.-B.; Xu, L. *Cryst. Growth Des.* **2005**, *5*, 65.

(3) (a) Ren, Y.-P.; Kong, X.-J.; Hu, X.-Y.; Sun, M.; Long, L.-S.; Huang, R.-B.; Zheng, L.-S. *Inorg. Chem.* **2006**, *45*, 4016. (b) Zheng, P. Q.; Ren, Y. P.; Long, L. S.; Huang, R. B.; Zheng, L. S. *Inorg. Chem.* **2005**, *44*, 1190.

(4) Hagrman, D.; Zubieta, C.; Rose, D. J.; Zubieta, J.; Haushalter, R. C. *Angew. Chem., Int. Ed.* **1997**, *36*, 873. Hagrman, D.; Hagrman, P. J.; Zubieta, J. *Angew. Chem., Int. Ed.* **1999**, *38*, 3165.

10.1021/ic061664y CCC: $33.50
Published on Web 12/02/2006

Scheme 1. Schematic View of the Approach to the Construction of Porous POMs-Based Coordination Polymers through Direct Incorporation between POMs and the Voids of a 2D Metal−Organic Network

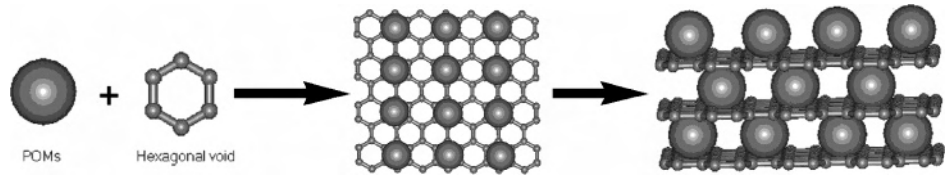

$(PMo_{12}O_{40})(H_2O)_{3.5}\}_n$ (2-Mepz = 2-methylpyrazine; **3**), $\{[Ag(2,3\text{-}Me_2pz)_{1.5}]_4(SiW_{12}O_{40})\}_n$ (**4**), $\{[Cu(pz)_{1.5}]_4(SiW_{12}O_{40})(H_2O)_3\}_n$ (pz = pyrazine; **5**), $\{[Cu(2,3\text{-}Me_2pz)_{1.5}]_4(SiW_{12}O_{40})\}_n$ (**6**), $\{[Cu(4,4'\text{-bipy})_{1.75}]_4(SiW_{12}O_{40})(H_2O)_2\}_n$ (**7**), and $\{[Cu_2(4,4'\text{-bipy})_4(H_2O)_4](SiW_{12}O_{40})(4,4'\text{-bipy})_2(H_2O)_4\}_n$ (**8**). We show not only that the construction of POMs-based coordination polymers through direct incorporation between POMs and the voids in the 2D network provides a convenient synthetic route to POMs-based open metal−organic frameworks but also that the pore of the material exhibits a unique flexibility.

We adopt the incorporation between POMs and the voids of the 2D metal−organic network to synthesize POMs-based metal−organic frameworks for the following reasons: First, if a 2D network with a suitable void was selected to cooperate with POMs, it is possible for POMs to occupy part of the voids in the 2D network[5] and act as pillar ligands to connect the adjacent 2D networks through electrostatic interaction between the POMs and the voids of the 2D network, generating a POMs-based open metal−organic framework (Scheme 1). Second, owing to the incorporation between the POMs and the voids of the 2D network being an electrostatic interaction, instead of coordination bonding, the difficulties encountered in the preparation of POMs-based coordination polymers through the approach of covalently linking POMs with metal−organic units could be overcome. Along this line, we chose the incorporation between Keggin-type POMs and the voids of two typical networks, 6^3 and 4^4 networks,[6] to assemble POMs-based open metal−organic frameworks.

Experimental Section

Materials and Methods. All of the reagents and solvents employed were commercially available and used as received without further purification. The C, H, and N microanalyses were carried out with a CE instruments EA 1110 elemental analyzer. The FT-IR spectra were recorded from KBr pellets in the range 4000−400 cm^{-1} with a Nicolet AVATAR FT-IR360 spectrometer. The thermogravimetric analysis (TGA), X-ray powder diffractometry (XRPD), and X-ray photoelectron spectroscopy (XPS) studies of the complexes were performed with a NETZSCH STA 449C instrument, with a Panalytical X-Pert pro diffractometer with Cu Kα radiation, and with a Physical Electrons Quantum 2000 Scanning Esca Microprob spectrometer, respectively.

Syntheses. A. $\{[Cu(2,3\text{-}Me_2pz)(2,5\text{-}Me_2pz)_{0.5}]_4(SiW_{12}O_{40})(2,5\text{-}Me_2pz)\}_n$ **(1).** $H_4SiW_{12}O_{40}$ (0.36 g, 0.125 mmol), 2,5-Me_2pz (0.108 g, 1.0 mmol), 2,3-M_2epz (0.05 mL, 0.2 mmol), and $Cu(NO_3)_2{\cdot}3H_2O$ (0.12 g, 0.5 mmol) were dissolved in 16 mL of distilled water with stirring at room temperature. When the pH value of the mixture was adjusted to ∼5−6 with 1.0 mol·L^{-1} NaOH, the cloudy solution was put into a 25 mL Teflon-lined Parr, heated to 170 °C for 50 h, and then cooled to 100 °C at a rate of 5 °C·h^{-1}. After remaining at 100 °C for 16 h, the mixture was cooled to room temperature at a rate of 3 °C·h^{-1}. Red crystals of **1** were obtained in 30.5% yield (based on the 2,3-Me_2pz ligand). Elemental anal. Calcd (found) for **1**: C, 12.97 (12.74); H, 1.44 (1.54); N, 5.05 (5.16). IR (KBr, cm^{-1}): 3448s, 2924w, 1637w, 1570s, 1452m, 1428 m, 1377w, 1311w, 1089s, 979m, 923s, 878m, 799s, 541m.

B. $\{[Cu_2(4,4'\text{-bipy})_4(H_2O)_4](SiW_{12}O_{40})(H_2O)_{18}\}_n$ **(2).** $H_4SiW_{12}O_{40}$ (1.14 g, 0.40 mmol), 4,4′-bipy (0.08 g, 0.5 mmol), and $CuCl_2{\cdot}2H_2O$ (0.85 g, 0.5 mmol) were dissolved in 20 mL of distilled water with stirring at room temperature. When the pH value of the mixture was adjusted to ∼5−6 with 1.0 mol·L^{-1} NaOH, the cloudy solution was put into a 25 mL Teflon-lined Parr, heated to 180 °C for 24 h, and then cooled to 100 °C at a rate of 5 °C·h^{-1}. After remaining at 100 °C for 10 h, the mixture was cooled to room temperature at a rate of 5 °C·h^{-1}. Purple-red crystals of **2** were obtained in 10.2% yield (based on the 4,4′-bipy ligand). Elemental anal. Calcd (found) for **2**: C, 12.0 (11.9); H, 1.93 (1.89); N, 2.79 (2.78). IR (KBr, cm^{-1}): 3435s, 2351m, 1613s, 1537w, 1417m, 1222m, 1073w, 1016w, 972s, 923vs, 882w, 796vs, 614w, 534m.

C. $\{[Cu(2\text{-}Mepz)_{1.5}]_3(PMo_{12}O_{40})(H_2O)_{3.5}\}_n$ **(3).** $H_3PMo_{12}O_{40}{\cdot}nH_2O$ (0.304 g, 0.167 mmol), 2-Mepz (0.25 mL, 1.0 mmol), and $Cu(NO_3)_2{\cdot}3H_2O$ (0.24 g, 1.0 mmol) were dissolved in 18 mL of distilled water with stirring at room temperature (pH = 3−4). The cloudy solution was put into a 25 mL Teflon-lined Parr, heated to 180 °C for 50 h, and then cooled to 100 °C at a rate of 5 °C·h^{-1}. After remaining at 100 °C for 34 h, the mixture was cooled to room temperature at a rate of 5 °C·h^{-1}. Black plate crystals of **3** were obtained in 40.6% yield (based on 2-Mepz). Elemental anal. Calcd (found) for **3**: C, 10.81 (10.57); H, 1.37 (1.45); N, 5.04 (4.92). IR (KBr, cm^{-1}): 2924s, 2853m, 2365w, 1629s, 1458m, 1400m, 1384m, 1157w, 1113w, 1064m, 960s, 868m, 797s, 669w, 593w, 498w.

D. $\{[Ag(2,3\text{-}Me_2pz)_{1.5}]_4(SiW_{12}O_{40})\}_n$ **(4).** $H_4SiW_{12}O_{40}$ (0.36 g, 0.125 mmol), 2,3-Me_2pz (1.08 g, 1.0 mmol), and $AgNO_3$ (0.34 g, 2.0 mmol) were dissolved in 16 mL of distilled water with stirring at room temperature (pH = 3−4). The cloudy solution was put into a 25 mL Teflon-lined Parr, heated to 180 °C for 50 h, and then cooled to 80 °C at a rate of 5 °C·h^{-1}. After remaining at 100 °C for 16 h, the mixture was cooled to room temperature at a rate of 5 °C·h^{-1}. Yellow block crystals of **4** were obtained in 20.5% yield (based on $H_4SiW_{12}O_{40}$). Elemental anal. Calcd (found) for **4**: C, 10.92 (10.49); H, 1.21 (1.51); N, 4.25 (3.81). IR (KBr, cm^{-1}): 3474s, 1628m, 1431w, 1407m, 1175m, 1014m, 974s, 923s, 880m, 799s, 539m, 474w.

(5) Lisnard, L.; Dolbecq, A.; Mialane, P.; Marrot, J.; Codjovi, E.; Secheresse, F. *Discuss. Faraday Soc*. **2005**, 3913.

(6) (a) MacGillivray, L. R.; Subramanian, S.; Zaworotko, M. J. *J. Chem. Soc., Chem. Commun*. **1994**, 1325. (b) Otieno, T.; Rettig, S. J.; Thompson, R. C.; Trotter, J. *Inorg. Chem.* **1993**, *32*, 1607. (c) Carlucci, L.; Ciani, G.; Proserpio, D. M.; Sironi, A. *J. Am. Chem. Soc.* **1995**, *117*, 4562. (d) Carlucci, L.; Cia, G.; Proserpio, D. M.; Sironi, A. *Inorg. Chem.* **1995**, *34*, 5698. (e) Noro, S.; Kitaura, R.; Kondo, M.; Kitagawa, S.; Ishii, T.; Matsuzaka, H.; Yamashita, M. *J. Am. Chem. Soc.* **2002**, *124*, 2568. (f) Lloret, F.; Munno, G. D.; Julve, M.; Cano, J.; Ruiz, R.; Caneschi, A. *Angew. Chem., Int. Ed.* **1998**, *37*, 135.

Table 1. Crystal Data and Details of Data Collection and Refinement for Complexes **1**−**8**

	1	**2**	**3**	**4**	**5**	**6**	**7**	**8**
formula	$C_{42}H_{56}Cu_4N_{14}O_{40}SiW_{12}$	$C_{40}H_{76}Cu_2N_8O_{62}SiW_{12}$	$C_{22.5}H_{34}Cu_3Mo_{12}N_9O_{43.5}P$	$C_{36}H_{48}Ag_4N_{12}O_{40}SiW_{12}$	$C_{24}H_{28}Cu_4N_{12}O_{42}SiW_{12}$	$C_{36}H_{48}Cu_4N_{12}O_{40}SiW_{12}$	$C_{70}H_{62}Cu_4N_{14}O_{43}SiW_{12}$	$C_{60}H_{63}Cu_2N_{12}O_{48}SiW_{12}$
mol wt	3885.46	4022.46	2499.46	3954.63	3645.03	3777.31	4275.79	4081.59
cryst syst	monoclinic	orthorhombic	rhombohedral	orthorhombic	triclinic	monoclinic	triclinic	orthorhombic
space group	*C*2/*m*	*Cccm*	$R\bar{3}m$	*Pbca*	$P\bar{1}$	$P2_1/c$	$P\bar{1}$	$Ccm2_1$
a/Å	17.385(3)	17.740(5)	20.225(3)	12.546(3)	11.818(2)	13.371(3)	11.280(3)	22.098(4)
b/Å	18.976(4)	22.157(6)		23.138(5)	12.130(2)	21.109(5)	14.974(4)	22.769(4)
c/Å	12.221(2)	22.245(6)	23.057(6)	23.471(5)	12.237(3)	14.088(3)	15.557(4)	16.907(3)
α/deg					114.618(3)		105.665(5)	
β/deg	114.319(3)				99.606(3)	118.33	102.262(5)	
γ/deg			120.00		95.554(3)		106.328(4)	
V/Å^3	3673.7(12)	8744(4)	8168(3)	6813(2)	1545.2(5)	3500.0(13)	2306.8(9)	8507(2)
Z	2	4	6	4	1	2	1	4
D_c/g cm^{-3}	3.513	3.056	3.049	3.855	3.917	3.584	3.078	3.187
μ/mm^{-1}	19.943	16.311	3.954	21.401	23.695	20.926	15.898	16.757
no. of data/params	3520/272	4277/315	1891/175	5448/475	5002/430	5657/475	8844/655	9476/615
θ range/deg	1.83−26.00	1.47−26.00	1.46−27.00	1.76−25.00	1.88−25.00	1.90−25.00	1.51−26.00	1.28−27.00
obs reflns	3346	4066	1783	5416	4229	5037	7018	8938
R1 [$I > 2\sigma(I)$]	0.0730	0.0507	0.0447	0.0965	0.0754	0.0798	0.0627	0.0404
wR2 (all data)	0.1485	0.1019	0.1354	0.2018	0.2083	0.1799	0.1564	0.0847

E. $\{[Cu(pz)_{1.5}]_4(SiW_{12}O_{40})\cdot 2H_2O\}_n$ **(5).** $H_4SiW_{12}O_{40}$ (1.44 g, 0.5 mmol), pz (0.24 g, 3.0 mmol), and $Cu(NO_3)_2\cdot 3H_2O$ (0.24 g, 1.0 mmol) were dissolved in 18 mL of distilled water with stirring at room temperature. When the pH value of the mixture was adjusted to ∼3.5 with 1.0 mol·L^{-1} NaOH, the cloudy solution was put into a 25 mL Teflon-lined Parr, heated to 200 °C for 50 h, and then cooled to 120 °C at a rate of 10 °C·h^{-1}. After remaining at 120 °C for 16 h, the mixture was cooled to room temperature at a rate of 3 °C·h^{-1}. The red sheet crystal was obtained in 80% yield (based on $Cu(NO_3)_2\cdot 3H_2O$). Elemental anal. Calcd (found) for **5**: C, 7.83 (8.01); H, 0.87 (0.92); N, 4.57 (4.65). IR (KBr, cm^{-1}): 3450s, 2926w, 2358m, 1623m, 1416m, 1156w, 1053m, 1019m, 973s, 922s, 882m, 793s, 541m, 476m.

F. $\{[Cu(2,3\text{-}Me_2pz)_{1.5}]_4(SiW_{12}O_{40})\}_n$ **(6).** $H_4SiW_{12}O_{40}$ (0.36 g, 0.125 mmol), 2,3-Me_2pz (0.108 g, 1.0 mmol), and $Cu(NO_3)_2\cdot 3H_2O$ (0.12 g, 0.5 mmol) were dissolved in 18 mL of distilled water with stirring at room temperature. When the pH value of the mixture was adjusted to ∼3−4 with 1.0 mol·L^{-1} NaOH, the cloudy solution was put into a 25 mL Teflon-lined Parr, heated to 180 °C for 34 h, and then cooled to 100 °C at a rate of 10 °C·h^{-1}. After remaining at 100 °C for 16 h, the mixture was cooled to room temperature at a rate of 3 °C·h^{-1}. The red sheet crystals were obtained in 85% yield (based on $Cu(NO_3)_2\cdot 3H_2O$). Elemental anal. Calcd (found) for **6**: C, 11.44 (11.54); H, 1.27 (1.39); N, 4.45 (4.37). IR (KBr, cm^{-1}): 3449s, 2925w, 1629m, 1437m, 1412m, 1182m, 1012m, 970s, 922s, 882m, 799s, 533m.

G. $\{[Cu(4,4'\text{-bipy})_{1.75}]_4(SiW_{12}O_{40})(H_2O)_3\}_n$ **(7).** $H_4SiW_{12}O_{40}$ (1.15 g, 0.4 mmol), *β*-alanine (0.05 g, 0.56 mmol), 4,4′-bipy (0.156 g, 1.0 mmol), and $Cu(NO_3)_2\cdot 3H_2O$ (0.12 g, 0.5 mmol) were dissolved in 18 mL of water with stirring at room temperature. When the pH value of the mixture was adjusted to ∼8 with 1.0 mol·L^{-1} $NH_3\cdot H_2O$, the cloudy solution was put into a 25 mL Teflon-lined Parr, heated to 160 °C for 24 h, and then cooled to room temperature at a rate of 5 °C·h^{-1}. The yellow crystals were obtained in 10% yield (based on $Cu(NO_3)_2\cdot 3H_2O$). Elemental anal. Calcd (found) for **7**: C, 19.56 (19.87); H, 1.49 (1.56); N, 4.56 (4.62). IR (KBr, cm^{-1}): 3444s, 2924w, 2852w, 1605s, 1414m, 1384w, 969m, 921s, 884w, 798s, 533m.

H. $\{[Cu_2(4,4'\text{-bipy})_4(H_2O)_4](SiW_{12}O_{40})(4,4'\text{-bipy})_2(H_2O)_4\}_n$ **(8).** $H_4SiW_{12}O_{40}$ (1.14 g, 0.40 mmol), 4,4′-bipy (0.08 g, 0.5 mmol), and $CuNO_3\cdot 3H_2O$ (0.20 g, 0.8 mmol) were dissolved in 20 mL of distilled water with stirring at room temperature. When the pH value of the mixture was adjusted to ∼7 with 1.0 mol·L^{-1} NaOH, the cloudy solution was put into a 25 mL Teflon-lined Parr, heated to 200 °C for 48 h, and then cooled to 100 °C at a rate of 5 °C·h^{-1}. After remaining at 100 °C for 10 h, the mixture was cooled to room temperature at a rate of 5 °C·h^{-1}. Blue block crystals of **8** were obtained in 34.7% yield (based on the 4,4′-bipy ligand). Elemental anal. Calcd (found) for **8**: C, 17.64 (17.91); H, 1.57 (1.88); N, 4.12 (4.98). IR (KBr, cm^{-1}): 3416s, 2924w, 1601s, 1410m, 1384s, 1219m, 1065w, 1014w, 973s, 926s, 885m, 800s, 535m.

In the syntheses of complexes **3**, **5**, and **6**, the oxidation state of copper was changed from a reactant copper(II) ion to a resultant copper(I) ion. Such a phenomenon was often observed in the reaction of a nitrogen-containing ligand with a copper(II) ion under hydrothermal conditions, and a lower pH value and higher temperature of the reaction were found to be an important factor influencing the oxidation change of the copper ion.[7] The oxidation state change of copper from a reactant copper(II) ion to a resultant copper(I) ion in complex **1** is probably associated with the pz ligand,[6a−d] while the change in oxidation of the copper(II) ion in **7** is related to the carboxylate group.[8]

X-ray Crystallography. Data collection was performed on a Bruker SMART Apex CCD diffractometer at 123 K for **3**, at 173 K for **1**, **2**, **5**, **6**, and **8**, and at 293 K for **4** and **7**. Absorption corrections were applied by using the multiscan program SADABS.[9] The structures were solved by direct methods, and non-hydrogen atoms were refined anisotropically by least-squares on F^2 using the SHELXTL program.[10] The hydrogen atoms of organic ligands were generated geometrically (C−H, 0.96 Å). Crystal data as well as details of data collection and refinement for the complexes are summarized in Table 1.

Results and Discussion

Description of Crystal Structures. Parts a, b, and c of Figure 1 illustrate the structure of the 6^3 network of [Cu(2,3-

(7) Zhang, X. M.; Fang, R. Q. *Inorg. Chem.* **2005**, *44*, 3955. Zhang, X. M. *Coord. Chem. Rev.* **2005**, *249*, 1201. Lu, J. Y.; Cabrera, B. R.; Wang, R.-J.; Li, J. *Inorg. Chem.* **1999**, *38*, 4608. Graham, P. M.; Pike, R. D.; Sabat, M.; Bailey, R. D.; Pennington, W. T. *Inorg. Chem.* **2000**, *39*, 121. Lu, J. Y. *Coord. Chem. Rev.* **2003**, *246*, 327.
(8) Tao, J.; Zhang, Y.; Tong, M. L.; Chen, X. M.; Yuen, T.; Lin, C. L.; Huang, X. Y.; Li, J. *Chem. Commun.* **2002**, 1342.
(9) Sheldrick, G. M. *SADABS 2.05*; University of Göttingen: Göttingen, Germany.
(10) *SHELXTL 6.10*; Bruker Analytical Instrumentation: Madison, WI, 2000.

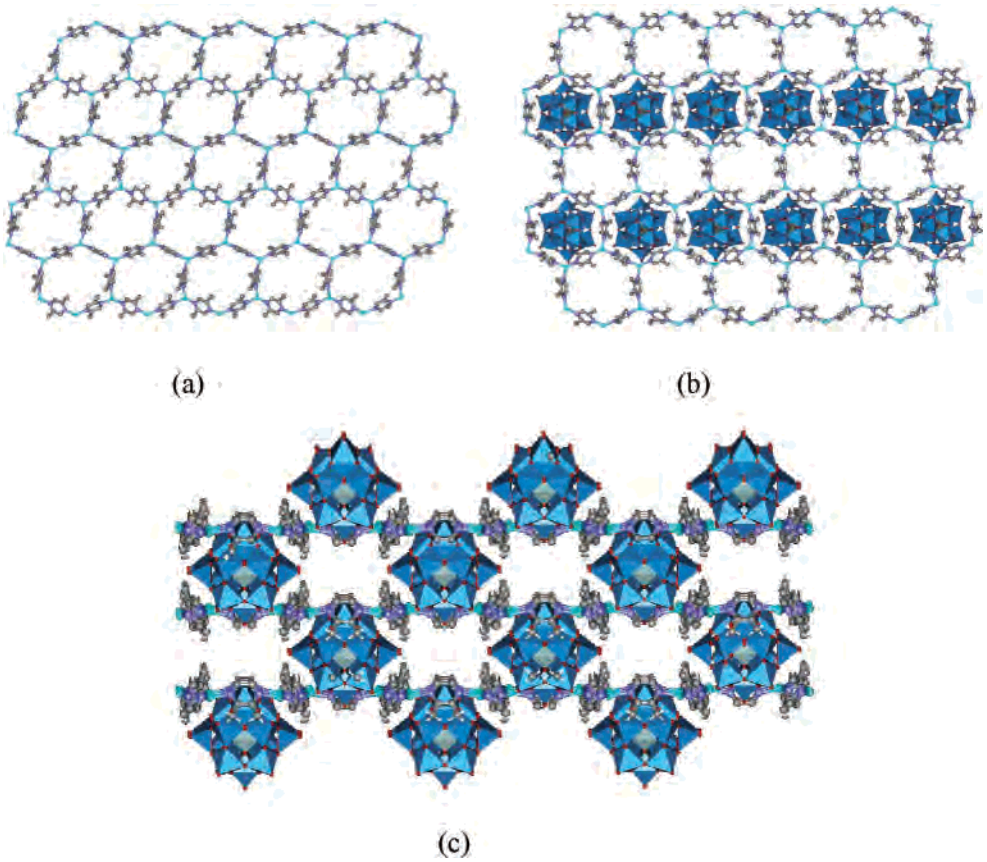

Figure 1. (a) Structure of the 6^3 network of $[Cu(2,3\text{-}Me_2pz)(2,5\text{-}Me_2pz)_{0.5}]_n^{n+}$ in **1**, (b) arrangement of the $SiW_{12}O_{40}^{4-}$ anion in the 6^3 network, and (c) structure of the 3D porous material of **1** (Cu, cyan; O, red; W, blue; Si, gray; C, gray; N, Cambridge blue).

$Me_2pz)(2,5\text{-}Me_2pz)_{0.5}]_n^{n+}$, the arrangement of the $SiW_{12}O_{40}^{4-}$ anion in the 6^3 network, and the structure of the 3D porous material of $\{[Cu(2,3\text{-}Me_2pz)(2,5\text{-}Me_2pz)_{0.5}]_4(SiW_{12}O_{40})(2,5\text{-}Me_2pz)\}_n$ (**1**), respectively. Each copper(I) cation tricoordinated by two 2,3-Me_2pz ligands and one 2,5-Me_2pz ligand, and each 2,3-Me_2pz and 2,5-Me_2pz ligand linked to two copper(I) cations through the coordination of the terminal nitrogen atom generate a 6^3 network, as shown in Figure 1a. The $SiW_{12}O_{40}^{4-}$ anion that is linearly and alternately arranged on the hexagonal voids in the 6^3 network (Figure 1b) results in a 3D structure with a 1D channel (Figure 1c) through the incorporation of the $SiW_{12}O_{40}^{4-}$ anions in one layer and the remaining voids from adjacent layers. The accessible porosity for the guest molecule (2,5-Me_2pz) calculated through the PLATON program[11] is 616.1 Å^3/mol (16.8%). The bond lengths of Cu−N are in the range 1.98(2)−2.06(2) Å, comparable to those of 1.971(4)−2.082(5) Å in the $\{[Cu^{I}(2,5\text{-}Me_2pz)_{1.5}](PF_6)\}_n$ complexes,[6b] while those of Si−O and W−O are 1.60(3)−1.63(2) and 1.680(15)−2.37(2) Å, respectively, comparable to those of 1.618(9)−1.643(12) and 1.698(12)−2.363(9) Å in the $[Ni_2(4,4'\text{-}Hbpy)_4(4,4'\text{-}bpy)(H_2O)_6](SiW_{12}O_{40})_2\cdot 16H_2O$ complex.[3b]

Complex **2** consists of two copper(II) cations, four 4,4′-bipy ligands, one $SiW_{12}O_{40}^{4-}$ anion, and twenty-two water molecules. Each copper(II) atom in **2** is six-coordinated by two water molecules at the apical positions and four nitrogen atoms from four 4,4′-bipy ligands, respectively, at the basal plane, forming a four-connected 2D structure of $[Cu(4,4'\text{-}bipy)_2(H_2O)_2]_n^{2n+}$, as illustrated in Figure 2a. $SiW_{12}O_{40}^{4-}$ anions alternately locate on the square voids of the 2D structure, generating a layer structure of $[Cu_2(4,4'\text{-}bipy)_4(H_2O)_4]_n\cdot(SiW_{12}O_{40})_n$ (Figure 2b). The two adjacent layers are further connected through the direct incorporation of the $SiW_{12}O_{40}^{4-}$ anion in one layer and the remaining voids in the adjacent layers, leading to a 3D structure of **2** (Figure 2c) with a two-dimensional $(H_2O)_{22}$ network (Figure 3) located in its cavity. The 2D $(H_2O)_{22}$ network can be viewed as an assembly of a $5^2 6^2 7^2$ cage-like $(H_2O)_{14}$ cluster and a $(H_2O)_4$ cluster. The bond lengths of Cu−N, Cu−O_{water}, Si−O, and W−O are 1.989(14)−2.008(14), 2.408(13)−2.865(11), 1.573(14)−1.72(2), and 1.684(9)−2.360(14) Å, respectively. The bond lengths of Si−O and W−O are comparable to those in **1**. Notably, the calculated accessible porosity of 3089.8 Å^3/mol (35.3%) for the water molecules in **2** is significantly larger than that of **1**, indicating that the void shape of the 2D network plays an important role in controlling the pore shape/size of the POMs-based coordination polymers.

Complex **3** consists of three copper(I) cations, four and a half 2-Mepz ligands, one $PMo_{12}O_{40}^{3-}$ anion, and three and a half water molecules. Each copper(I) center tricoordinated by three 2-Mepz ligands and each 2-Mepz ligand linked to two copper(I) cations through the coordination of its terminal nitrogen atom form a 6^3 network very similar to that in **1** (Figure 4a). Owing to the charge difference between

(11) Spek, A. L. *Acta Crystallogr., Sect. A* **1990**, *46*, C34.

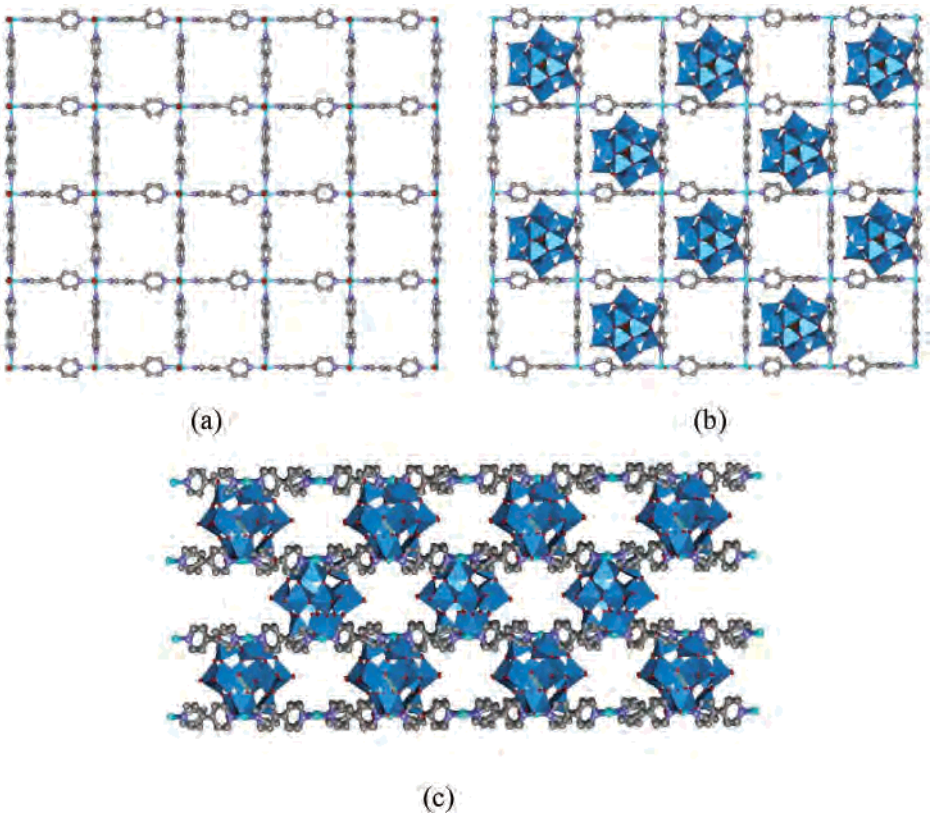

Figure 2. (a) Structure of the 4^4 network of $[Cu(4,4'\text{-bipy})_2(H_2O)_2]_n^{2+}$ in **2**, (b) arrangement of the $SiW_{12}O_{40}^{4-}$ anion in the 4^4 network in **2**, and (c) 3D structure of **2** (Cu, cyan; O, red; W, blue; Si, gray; C, gray; N, Cambridge blue).

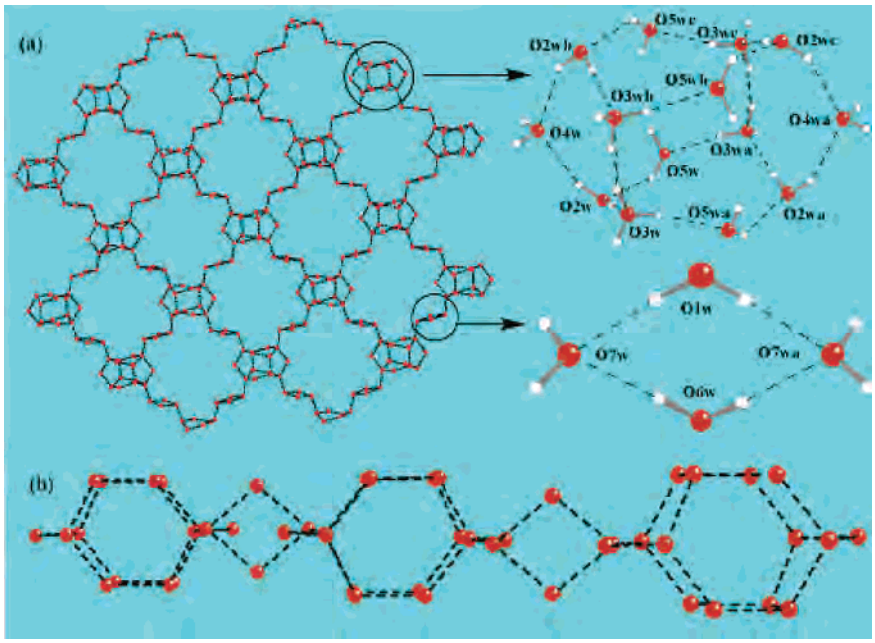

Figure 3. (a) 2D water network of $(H_2O)_{22}$ in **2** and (b) side view of (a).

$PMo_{12}O_{40}^{3-}$ and $SiW_{12}O_{40}^{4-}$, the incorporation of the $PMo_{12}O_{40}^{3-}$ anion into the 6^3 network leads to the $PMo_{12}O_{40}^{3-}$ anion occupying two-thirds of the voids in the 6^3 network in **3** (Figure 4b), instead of half of the voids as in **1** and **2**. As a result, the 3D structure of **3** is much different from that of **1** and **2** (Figure 4c). The bond lengths of Cu−N, P−O, and Mo−O are 1.964(5)−2.002(4), 1.529(6)−1.532(3), and 1.683(3)−2.435(2) Å, respectively. The bond length of Cu−N is comparable to that of **1**, while the bond lengths of P−O and Mo−O are comparable to those of 1.494(7)−1.532(7) and 1.637(8)−2.472(10) Å, respectively, in the $[Cu_3(2,3\text{-}Me_2pz)_3(PMo_{12}O_{40})]$ complex.[3a] The accessible porosity of 210.7 $Å^3$/mol (2.6%) for the guest molecule in **3** indicates that the charge of the POMs is important for modifying the pore shape/size of POMs-based coordination polymers.

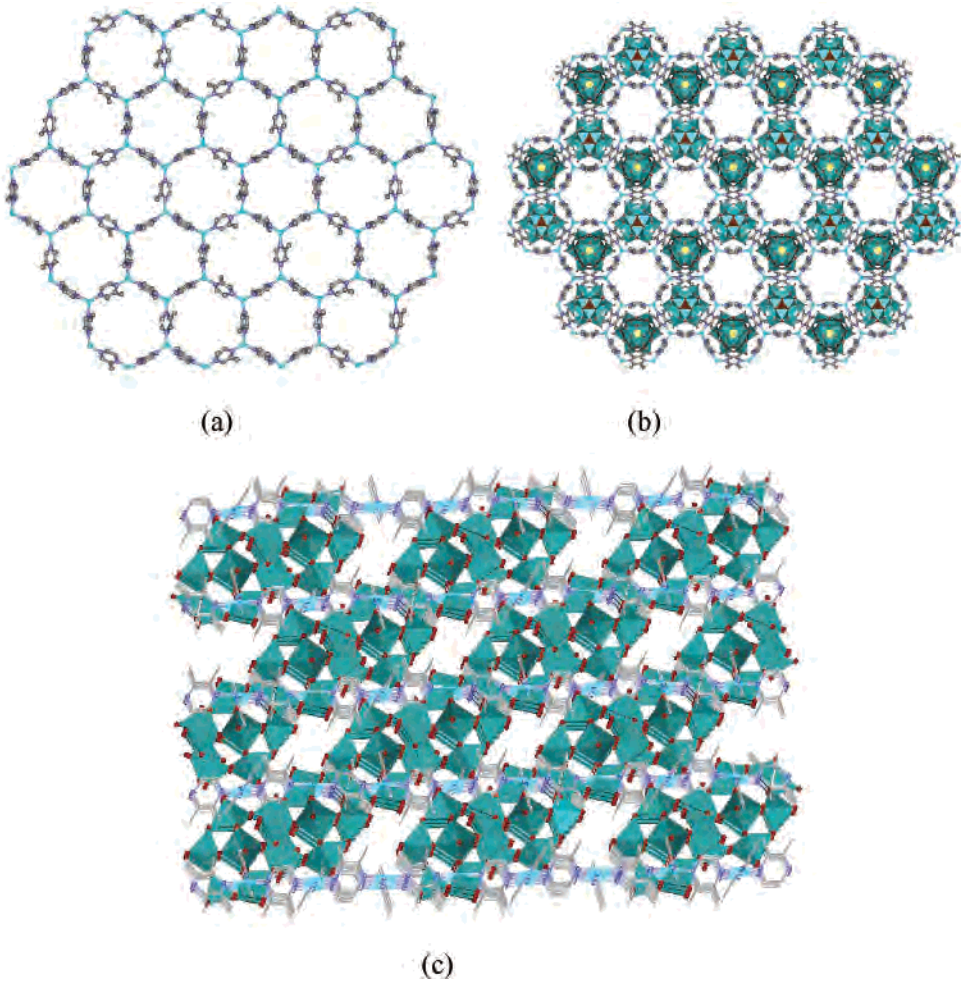

Figure 4. (a) Structure of the 6^3 network of $[Cu(2\text{-}Mepz)_{1.5}]_n^{n+}$ in **3**, (b) arrangement of the $PMo_{12}O_{40}^{3-}$ anion in the 6^3 network in **3**, and (c) 3D structure of **3** (Cu, cyan; O, red; Mo, green; P, orange; C, gray; N, Cambridge blue).

Complex **4** consists of four silver(I) cations, six 2,3-Me_2pz ligands, and one $SiW_{12}O_{40}^{4-}$ anion. Each silver(I) center tricoordinated by three 2,3-Me_2pz ligands and each 2,3-Me_2pz ligand bridged with two copper(I) cations generates a wavelike 6^3 network similar to that of $\{[Ag(pz)_{1.5}]\cdot(BF_4)\}_n$[5c] (Figure 5a). The incorporation of the $SiW_{12}O_{40}^{4-}$ anion results in the $SiW_{12}O_{40}^{4-}$ anion being linearly arranged on the hexagonal voids of the 2D network at two-row intervals (Figure 5b) and generates a 3D structure of **4** (Figure 5c) that is much different from that of **1** and **3**. The bond lengths of Ag−N, Si−O, and W−O are 2.20(3)−2.39(3), 1.495(9)−1.509(9), and 1.67(3)−2.48(3) Å, respectively. The bond lengths of Ag−N are comparable to those of 2.245(2)−2.419(3) Å in the $\{[Ag(pz)_{1.5}]\cdot(BF_4)\}_n$ complex,[6c] while the bond lengths of Si−O and W−O are comparable to those in **1** and **2**. In complex **4**, the accessible porosity for the guest molecule is 313.3 $Å^3$/mol (4.6%), showing the role of the metal ion radius in the 2D network in modifying the pore shape/size of POMs-based coordination polymers.

Complex **5** consists of four copper(I) cations, six pz ligands, one $SiW_{12}O_{40}^{4-}$ anion, and two water molecules. Similar to those in **1** and **3**, each copper(I) center in **5** is tricoordinated by three pz ligands and each pz ligand is coordinated by two copper(I) centers. However, the 2D structure in **5** is entirely different from those of **1** and **3**. As shown in Figure 6a, the 2D structure in **5** exhibits a unique 4^18^2 network with each copper(I) center surrounded by one square void and two octagonal voids, respectively. The $SiW_{12}O_{40}^{4-}$ anion in **5** is in the octagonal voids (Figure 6b) instead of on the voids of the 2D network as in **1**−**4**. As a result, the $SiW_{12}O_{40}^{4-}$ anion functionalizes an interpenetrating ligand to connect the square voids of the adjacent 2D networks, generating a 3D interpenetrating structure, as shown in Figure 6c. It was noted that, having never found a report of a 4^18^2 network in pz−copper(I) complexes in the Cambridge Structural Database (CSD),[11] the formation of a 4^18^2 network in **5** is related to the template of $SiW_{12}O_{40}^{4-}$. The bond lengths of Cu−N, Si−O, and W−O are 1.87(2)−1.934(17), 1.492(8)−1.523(9), and 1.667(18)−2.498(18) Å, respectively, compared to those in **1**.

Complex **6** consists of four copper(I) cations, six 2,3-Me_2pz ligands, and one $SiW_{12}O_{40}^{4-}$ anion. In fact, complex **6** can be viewed as a structural isomer of **5**. The bond lengths of Cu−N, Si−O, and W−O are 1.931(11)−1.996(12), 1.494(8)−1.508(7), and 1.629(16)−2.458(17) Å, respectively, compared to those in **5**.

Complex **7** consists of four copper(I) cations, seven 4,4′-bipy ligands, one $SiW_{12}O_{40}^{4-}$ anion, and two water mol-

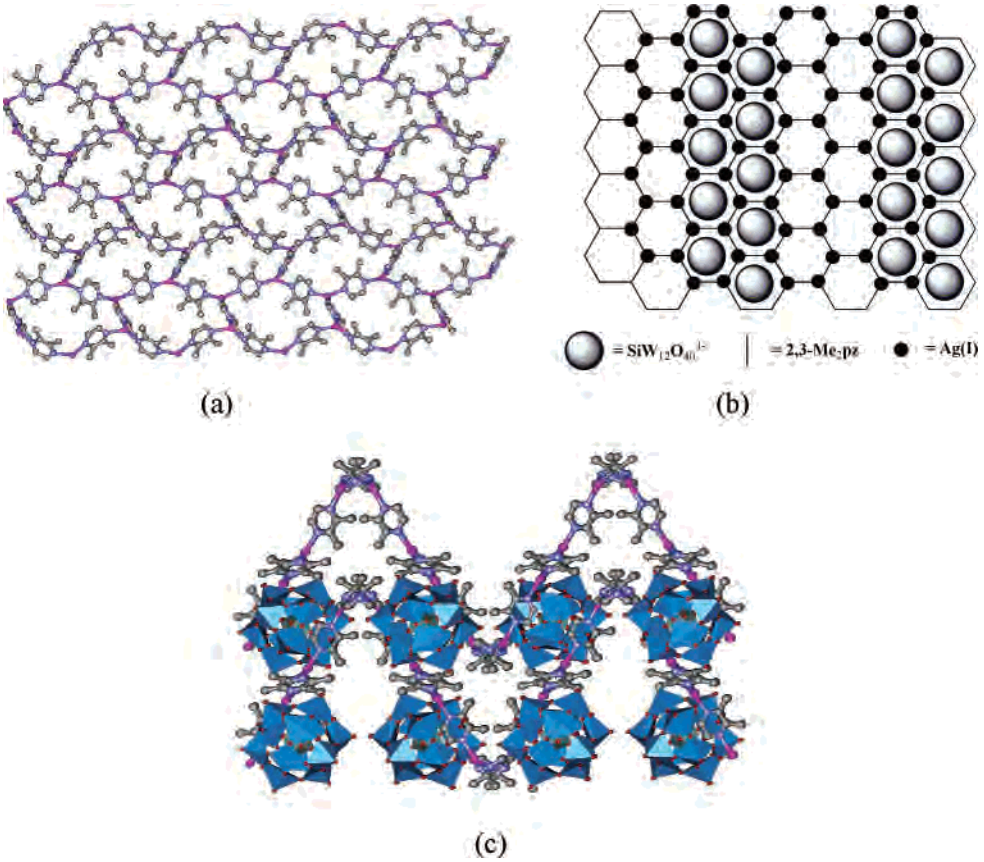

Figure 5. (a) Structure of the 6^3 network of $[Cu(2,3\text{-}Me_2pz)_{1.5}]_n^{n+}$ in **4**, (b) arrangement of the $SiW_{12}O_{40}^{4-}$ anion in the 6^3 network in **4**, and (c) 3D structure of **4** (Ag, purple; O, red; W, blue; Si, gray; C, gray; N, Cambridge blue).

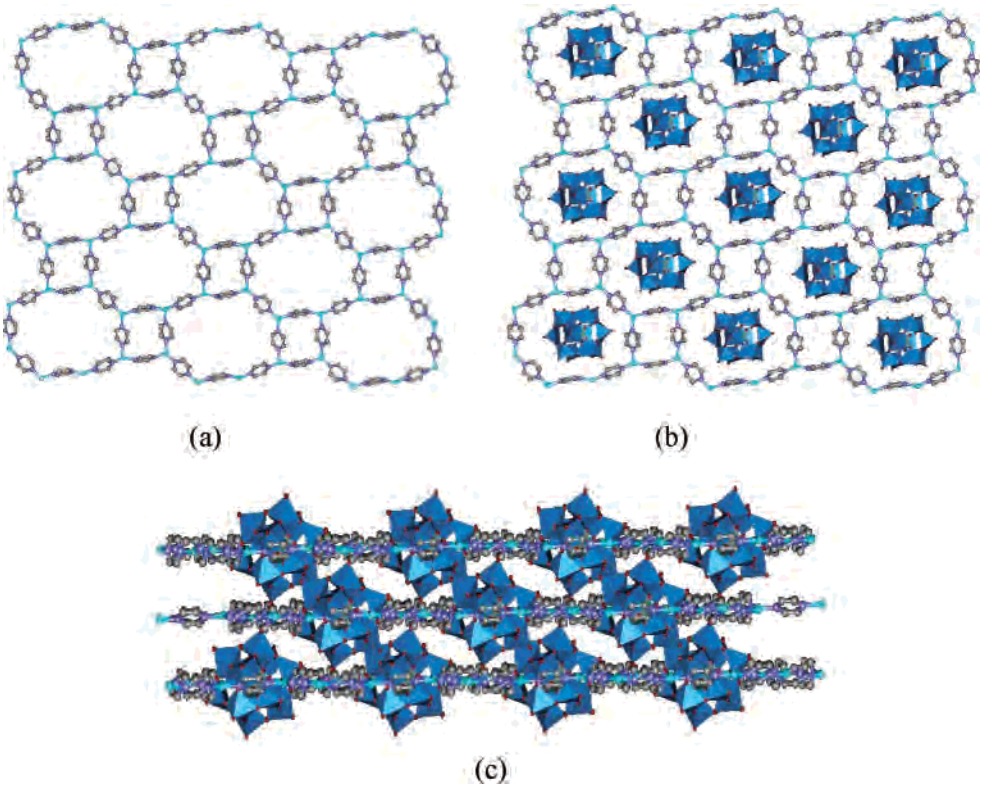

Figure 6. (a) Structure of the 4^18^2 network of $[Cu(pz)_{1.5}]_n^{n+}$ in **5**, (b) arrangement of the $SiW_{12}O_{40}^{4-}$ anion in the 4^18^2 network in **5**, and (c) 3D structure of **5** (Cu, cyan; O, red; W, blue; Si, gray; C, gray; N, Cambridge blue).

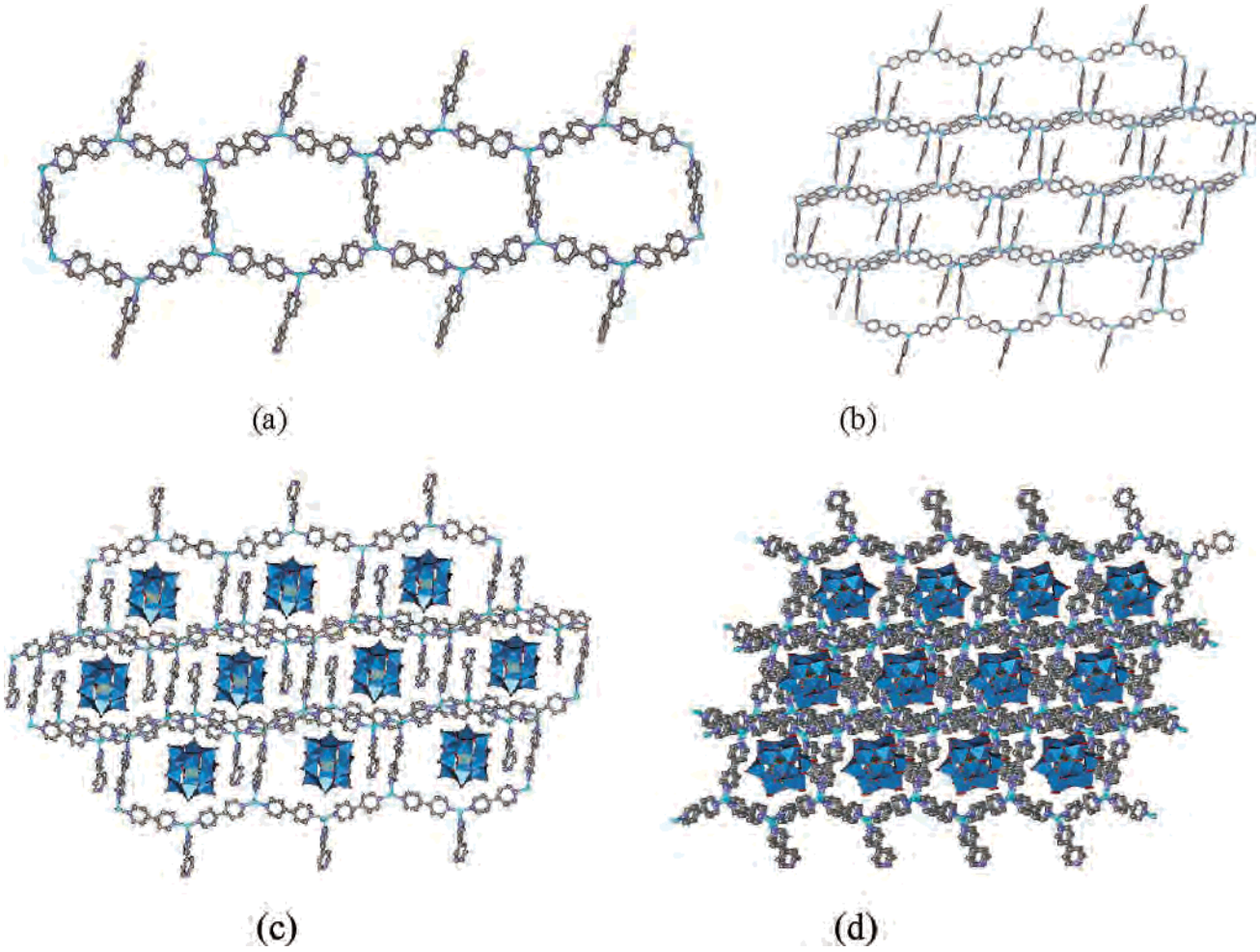

Figure 7. (a) Structure of the 1D chain of $\{[Cu(4,4'\text{-bipy})_{1.75}]_4\}_n^{4n+}$ in **7**, (b) structure of the pseudo-6^3 network of $[Cu(4,4'\text{-bipy})_{1.75}]_n^{n+}$ in **7**, (c) arrangement of the $SiW_{12}O_{40}^{4-}$ anion in the 2D network in **7**, and (d) 3D structure of **7** (Cu, cyan; O, red; W, blue; Si, gray; C, gray; N, Cambridge blue).

ecules. Crystal structure analysis reveals that there are two independent copper(I) centers in **7**: one is tricoordinated by three bridging 4,4′-bipy ligands, and the other is tricoordinated by two bridging 4,4′-bipy ligands and one monocoordinated 4,4′-bipy ligand. This linking mode leads to the formation of a unique 1D chain of $\{[Cu(4,4'\text{-bipy})_{1.75}]_4\}_n^{4n+}$ with hexagonal voids (Figure 7a), further confirming the template of $SiW_{12}O_{40}^{4-}$ in the assembly process, since a survey of the CSD[12] revealed that such a hexagonal void structure has not been found in copper(I or II)−4,4′-bipy complexes so far. Interlocking the adjacent chains through the monocoordinated 4,4′-bipy ligand generates a pseudo-6^3 network, as shown in Figure 7b. Similar to those in **5** and **6**, the $SiW_{12}O_{40}^{4-}$ anion locates in the voids of the 2D network (Figure 7c) and functionalizes the interpenetrating ligand to connect the adjacent 2D network, generating a 3D interpenetrating structure, as illustrated in Figure 7d. The bond lengths of Cu−N, Si−O, and W−O are 1.974(13)−2.114(13), 1.510(8)−1.526(8), and 1.695(12)−2.464(15) Å, respectively, compared to those in **1**, **5**, and **6**. In comparison with the copper(II)−4,4′-bipy network in **2** that exhibits a square void, the copper(I)−linear ligand networks in **1**, **3**, **5**, and **7** that show a hexagonal void are related to the coordination geometry of copper(I) that often locates in a three-coordinate geometry.[6a,b]

(12) *Cambridge Structural Database*, version 5.27; The Cambridge Crystallographic Data Centre: Cambridge, England, Aug 2006.

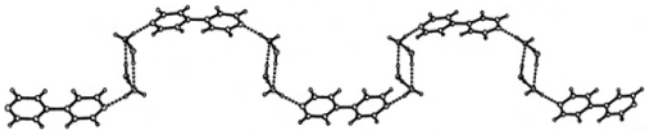

Figure 8. 1D chain of $[(H_2O)_4(4,4'\text{-bipy})]_n$ in **8**.

Crystal structural analysis reveals that complex **8** is a structural isomer of complex **2**. The only difference between **2** and **8** is the guest molecules. Instead of forming a $\{(H_2O)_{22}\}_n$ network as in **2**, the guest in **8** exhibits a 1D chain of $[(H_2O)_4(4,4'\text{-bipy})]_n$, as shown in Figure 8. The bond lengths of Cu−N, Si−O, and W−O are 1.986(6)−2.131(8), 1.539(6)−1.570(6), and 1.677(9)−2.424(5) Å, respectively, compared to those in **2**. Interestingly, the guest replacement not only results in the layer distance in **8** (8.50 Å) being significantly shorter than that in **2** (8.87 Å) but also leads to the calculated accessible porosity for the guest molecules in **8** (2681.5 $Å^3$/mol, 31.5%) being much smaller than that in **2**. Since there is no interaction between the 4,4′-bipy guest and the host in **8**, while the Cu−N bond distances in **8** are comparable to those in **2**, the fact that the pore size of the

coordination polymer is sensitive to the guest molecules is attributed to the electrostatic incorporation between POMs and the voids in the 2D network.[13]

It was noted that, based on the structures of **1**−**8**, it is clear that the relationship between the size of the void in the 2D network and that of the POM is of key importance for a successful assembly of porous POMs-based coordination polymers. During the investigation of the size of the void in different frameworks, we found that only when the size (van der Waals) of the void in the 2D network is smaller than that of the POM could the incorporation between the POM and the void of the 2D network effectively form porous POMs-based coordination polymers, since, in this case, the POM is located on the void of the 2D network and acts as a pillar ligand to connect adjacent 2D networks, as demonstrated with complexes **1**−**4** and **8**. Otherwise, the POM would locate in the void of the 2D network and functionalize an interpenetrating ligand to connect the adjacent 2D networks, generating a 3D interpenetrating POMs-based coordination polymer, as shown in complexes **5**, **6**, and **7**.

Spectroscopic Characterization. Complexes **2**, **3**, and **7** were selected to investigate the oxidation of the W or Mo atom. X-ray photoelectron spectroscopies (Supporting Information, Figure 1S) reveal that the W ($4f_{7/2}$) binding energies in **2** and **7** are 35.2 and 35.4 eV, respectively, while the Mo binding energy in **3** is 232.9 eV, indicating that the oxidation state of W and Mo in the complexes is +6.[14] These results are consistent with the crystal structure analyses.

TG Analysis and XPRD Study of 8. Complex **8** was selected to investigate its thermal stability in nitrogen-gas and air atmospheres. In a nitrogen-gas atmosphere (Figure 9a), complex **8** displays an initial weight loss of 5.5% between 25 and 240 °C. This is significantly higher than that of 3.5% calculated for the release of the lattice water and coordination water molecules, indicating that part of the 4,4′-bpy guest was released in the 25−240 °C temperature range. The second weight loss covered a temperature range from ∼320 to 380 °C; the weight loss of 5.9% is much lower than that of 7.7% calculated for the loss of two 4,4′-bpy guests. The total weight loss of 11.4% before 380 °C is very close to that of 11.2% calculated for the release of eight water molecules and two 4,4′-bpy guests, further confirming that part of the 4,4′-bpy guest was released before 240 °C. No evident weight loss between 242 and 311 °C indicates that complex **8** possesses a relatively higher thermal stability. At temperatures higher than 380 °C, complex **8** was slowly decomposed, and it became a tungstosilicate at 800 °C (the experimental weight loss of 27.4% is slightly higher than that of 26.5% calculated for the weight loss of the water molecules and organic ligands in complex **8**). In an air atmosphere, however, the thermal stability of complex **8** is rather poor. As shown in Figure 9b, complex **8** displays an initial weight loss of 3.4% between 25 and 104 °C, corresponding to the weight loss of the guest and coordinated water molecules (calculated, 3.5%). The second weight loss covered a temperature range from ∼104 to 253 °C; the weight loss of 7.5% is very close to that of 7.7% calculated for the loss of four 4,4′-bpy guests. At temperatures higher than 253 °C, complex **8** was rapidly decomposed, and it became a mixture of Cu_2SiO_4, WO_2, and WO_3 at 800 °C (the experimental weight loss of 41.6% is significantly higher than that of 26.5% calculated for the weight loss of the water molecules and organic ligands in complex **8**).

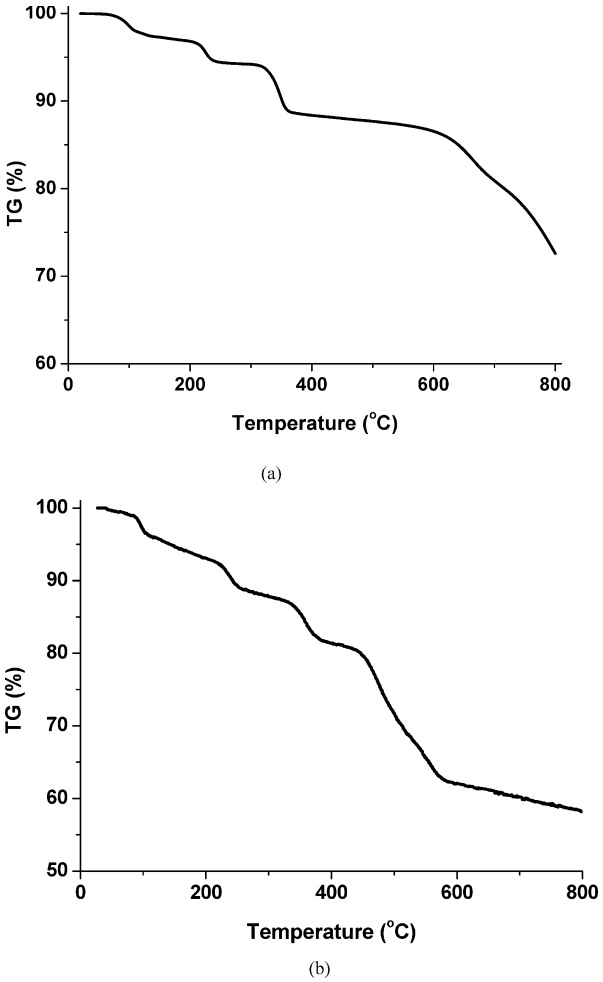

Figure 9. TGA curve for **8** over the temperature range ∼25−800 °C (a) in a nitrogen-gas atmosphere and (b) in air.

XRPD patterns at different conditions for complex **8** are shown in Figure 10. In comparison with that of **8** at 25 °C, the XRPD pattern of **8** at 150 °C (namely **8a**) shows very different peaks. Combined with the TG analysis in air, it is reasonable to conclude that all of the water molecules and part of the 4,4′-bpy guest in **8** were released from the framework at this temperature. At 200 °C, the XRPD pattern of **8** (namely **8b**) is further changed and is significantly different from that of **8a**, indicating that the 4,4′-bpy guest was further released from the framework. Interestingly, based on the XRPD patterns of **8a** and **8b** exposed to air, it was found that the reloading of the guest molecules into the framework formed through electrostatic incorporation is much slower than the reloading of the guest molecules into

(13) Johnson, B. J. S.; Geers, S. A.; Brennessel, W. W.; Young, V. G.; Stein, A. *J. Chem. Soc., Dalton Trans.* **2003**, 4678. Lisnard, L.; Dolbecq, A.; Mialane, P.; Marrot, J.; Codjovi, E.; Sécheresse, F. *Dalton Trans.* **2005**, 3913. Knaust, J. M.; Inman, C.; Keller, S. W. *Chem. Commun.* **2004**, 492.

(14) Luan, G. Y.; Li, Y. G.; Wang, S. T.; Wang, E. B.; Han, Z. B.; Hu, C. W.; Hu, N. H.; Jia, H. Q. *J. Chem. Soc., Dalton Trans.* **2003**, 233.

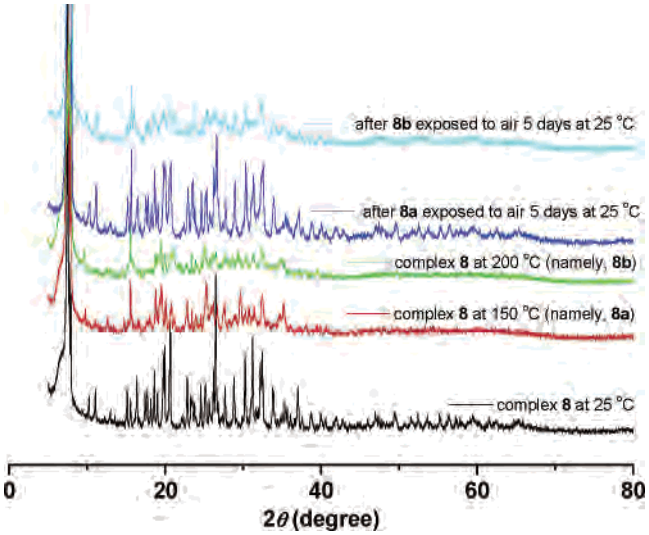

Figure 10. XPRD patterns of **8** at different temperatures.

the porous materials formed through coordination bonding, and the more the guest is released, the slower the reloading of the guest. For example, at 25 °C, it takes 5 days for **8a** to reload the water molecules, while, under the same conditions (at 25 °C, 5 days), the amount of guest reloaded into **8b** is much less than that reloaded into **8a**. This unique guest reloading behavior is attributed to the electrostatic incorporation in the framework. As we know, owing to the incorporation in the framework being an electrostatic interaction, the guest release would increase the electrostatic interaction between POMs and the 2D network and decrease the pore volume of the framework, and the more the guest is released, the smaller the pore volume of the framework and the bigger the electrostatic interaction between POMs and the 2D network. Thus, the more the guest is released, the more difficult it is for the guest to be reloaded.

Conclusions

POMs-based metal−organic frameworks represent an outstanding class of functional materials[15] and are regarded as green materials.[16] We noted that several POMs-based open metal−organic frameworks have been synthesized through the coordination of POMs to a metal−organic unit or by embedding POMs into a 3D metal−organic framework in the past decade.[4,17−19] In this work, we, based on direct incorporation between POMs and the voids in the 2D metal−organic network, have synthesized a series of 3D POMs-based coordination polymers, revealing that the relationship between the size of the void of the 2D network and that of the POMs is of key importance for the successful synthesis of POMs-based open metal−organic frameworks. Guest replacement shows that the pore size of the material constructed through direct incorporation between POMs and the voids of the 2D network is very sensitive to guest molecules. Together with the efficiency of the approach in precisely controlling the material pore size/shape, it is reasonable to believe that the present work is important to expand the application of POMs-based materials.

Acknowledgment. We thank the NNSFC (Grant Nos. 20471050, 20271044, and 20423002), the Ministry of Education Key Project (104201), and the NSF of Fujian province (E0410005) for financial support.

Supporting Information Available: X-ray crystallographic files in cif format for complexes **1**−**8** (CCDC numbers 605283−605290) and X-ray photoelectron spectra for complexes **2**, **3**, and **7**. This material is available free of charge via the Internet at http://pubs.acs.org.

IC061664Y

(15) Sadakane, M.; Dickman, M. H.; Pope, M. T. *Angew. Chem., Int. Ed.* **2000**, *39*, 2914. Zhang, X. M.; Tong, M. L.; Feng, S. H.; Chen, X. M. *J. Chem. Soc., Dalton Trans.* **2001**, 2069. Zheng, L.-M.; Wang, Y.-S.; Wang, X.-Q.; Korp, J. D.; Jacobson, A. J. *Inorg. Chem.* **2001**, *40*, 1380. Kortz, U. *Angew. Chem., Int. Ed.* **2002**, *41*, 4070. Kang, J.; Xu, B.-B.; Peng, Z.-H.; Zhu, X.-D.; Wei, Y.-G.; Powell, D. R. *Angew. Chem., Int. Ed.* **2005**, *44*, 6902. An, H.-Y.; Wang, E.-B.; Xiao, D.-R.; Li, Y.-G.; Su, Z.-M.; Xu, L. *Angew. Chem., Int. Ed.* **2006**, *45*, 904. Ren, Y. P.; Kong, X. J.; Long, L. S.; Huang, R. B.; Zheng, L. S. *Cryst. Growth Des.* **2006**, *6*, 572. Chen, J. X.; Lan, T. Y.; Huang, Y. B.; Wei, C. X.; Li, Z. S.; Zhang, Z. C. *J. Solid State Chem.* **2006**, *179*, 1904.

(16) Misono, M. *Chem. Commun.* **2001**, 1141.

(17) Inman, C.; Knaust, J. M.; Keller, S. W. *Chem. Commun.* **2002**, 156. Liu, S.-X.; Xie, L.-H.; Gao, B.; Zhang, C.-D.; Sun, C.-Y.; Li, D.-H.; Su, Z.-M. *Chem. Commun.* **2005**, 5023. Lu, Y.; Li, Y.-G.; Wang, E.-B.; Lu, J.; Xu, L.; Clérac, R. *Eur. J. Inorg. Chem.* **2005**, *7*, 1239.

(18) Hagrman, P. J.; Hagrman, D.; Zubieta, J. *Angew. Chem., Int. Ed.* **1999**, *38*, 2638. Finn, R. C.; Rarig, R. S., Jr.; Zubieta, J. *Inorg. Chem.* **2002**, *41*, 2109. Burkholder, E.; Golub, V.; O'Connor, C. J.; Zubieta, J. *Inorg. Chem.* **2003**, *42*, 6729. Burkholder, E.; Golub, V.; O'Connor, C. J.; Zubieta, J. *Chem. Commun.* **2003**, 2128. Burkholder, E.; Wright, S.; Golub, V.; O'Connor, C. J.; Zubieta, J. *Inorg. Chem.* **2003**, *42*, 7460. Khan, M. I.; Yohannes, E.; Nome, R. C.; Ayesh, S.; Golub, V. O.; O'Connor, C. J.; Doedens, R. J. *Chem. Mater.* **2004**, *16*, 5273. Burkholder, E.; Golub, V.; O'Connor, C. J.; Zubieta, J. *Inorg. Chem.* **2004**, *43*, 7014. Armatas, N. G.; Burkholder, E.; Zubieta, J. *J. Solid State Chem.* **2005**, *178*, 2430.

(19) Yang, L.; Naruke, H.; Yamase, T. *Inorg. Chem. Commun.* **2003**, *6*, 1020.